Supplemental materials for

Saccharomyces cerevisiae depend on vesicular traffic between Golgi and vacuole when Inositolphosphorylceramide synthase Aur1 is inactivated

Supplemental Materials and methods

When indicated, medium was supplemented with Aureobasidin A (Takara Biomedicals, Shiga, Japan), Australifungin (a generous gift from Merck Sharp & Dohme), cycloheximide, Myriocin, Doxycycline, or inositol (Sigma). Rabbit antibody detecting phosphorylated Slt2 (Phospho-p44/42 MAPK (Erk1/2) (Thr202/Tyr204) (20G11) Rabbit mAb #4376) was from Cell Signalling Technology; antibodies against Ypk1 phosphorylated at Thr662 were a kind gift of Robbie Loewith, Geneva University, Switzerland. Monomethylamine (33% in ethanol) was from Fluka AG, Buchs, Switzerland. BODIPY 493/503 was obtained from Invitrogen, Carlsbad, CA. [^{14}C]-serine (ARC 0676 in 2% EtOH) and [^{3}H]-*myo*-inositol (ART 0116B in 10% EtOH) were from ARC.

Quinacrine staining for vacuolar acidification. Cells were grown in YPD at 30°C to an OD_{600} of 0.8-1.2. Cells were grown for 1 h with or without AbA (0.25 µg/ml). Thereafter, 3 OD_{600} units of cells were collected, resuspended in 100 µl sterile staining buffer (YPD pH 7.6, 100 mM HEPES, 200 µM Quinacrine, added from stock in water) and left for 8 min at 30°C. Cells were washed 3 times with 1 ml of wash buffer (100 mM HEPES pH 7.6, 0.2% glucose), once at RT, two times at 4°C (3000 x g, 1 min) and then kept on ice in wash buffer. Cells were viewed under UV and visible light using an FITC filter. All pictures of were taken under exactly the same conditions, one stack was photographed with 300 ms exposition, only 1 picture/slide was taken to avoid quenching and at least 3 slides/cell type and condition were

photographed. All pictures were taken within 12 to 60 min of Quinacrine staining and no changes were observed during this time interval.

Supplemental Tables

Table S1. Yeast *Saccharomyces cerevisiae* strains

Strains	Genotype	Reference
BY4742	*MAT*α *his3Δ1 leu2Δ0 lys2Δ0 ura3Δ0*	EUROSCARF, (Frankfurt, GE)
yyΔΔ (FBY2182)	BY4742 but *ypc1Δ::kanMX ydc1Δ::kanMXΔ::natMX4*	(24)
FBY5313	*MAT*α *can1Δ::STE2pr-Sp_his5 lyp1Δ his3Δ1 leu2Δ0::loxP-LEU2-loxP ura3Δ0 met15Δ0*	C. Boone
tetAUR1 (FBY5318)	*MAT*α *can1Δ::STE2pr-Sp_his5 lyp1Δ his3Δ1 leu2Δ0::loxP-LEU2-loxP ura3Δ0 met15Δ0 tetO2-AUR1::natMX4*	This study
tetAUR1.URA3 (FBY5332)	As tetAUR1 but also containing pNP302	This study
vma2Δ.tetAUR1.URA3 (FBY2471)	As FBY5332 but *vma2Δ::kanMX*	This study
vma11Δ.tetAUR1.URA3 (FBY2467)	*MAT***a**, *CAN1 tetO2-AUR1::natMX4 vma11Δ::kanMX* (obtained by crossing with FBY5332)	This study
tetAUR1.YPC1 (FBY5333)	As tetAUR1 but also containing pYPC1-URA3	This study
vma11Δ.tetAUR1.YPC1 (FBY2475)	As FBY5333 but *vma11Δ::kanMX*	This study
WT.URA3 (FBY2470)	*MAT*α *can1Δ::STE2pr-Sp_his5 AUR1 VMA11* (derived from cross of BY4741 *vma11::kanMX* and tetAUR1.URA3 (FBY5332))	This study
vma11Δ.WT.URA3 (FBY2468)	*MAT*α *CAN1 AUR1 vma11::kanMX* (derived from cross of BY4741 *vma11::kanMX* and tetAUR1.URA3 (FBY5332))	This study
tetAUR1.GAL-vector (FBY5331)	As tetAUR1 but also containing pBF841	This study
tetAUR1.GAL-YPC1 (FBY5330)	As tetAUR1 but also containing pBF842	This study
tetAUR1.GAL-YPC1* (FBY5336)	As tetAUR1 but also containing pBF847	This study
tetAUR1.GAL-YPC1** (FBY5337)	As tetAUR1 but also containing pBF843	This study
FBY5334	*MAT*α *his3Δ1 leu2Δ0 lys2Δ0 ura3Δ0 ypc1::kanMX4 ydc1::kanMX4::natMX dpl1::URA3MX*	This study
FBY5335	*can1Δ::STE2pr-Sp_his5 or CAN1 lyp1Δ or LYP1 his3Δ1 leu2Δ0 ura3Δ0 met15Δ0 sur2Δ::kanMX ydc1Δ::natMX ypc1Δ::leu2*	This study
cog6Δ.tetAUR1	tetAUR1 but *cog6::kanMX*	This study
aalΔΔΔ.GDGA1 (RSY32	*MAT***a** *his3Δ1, leu2Δ0 lys2Δ0 ura3Δ0*	(68)

92)	*trp1::URA3 are1:: KanMX are2::KanMX lro1::loxP GAL1-GFP-DGA1-HIS3*	
aadΔΔΔ.GLRO1 (RSY3202)	*MAT*α *his3Δ1 leu2Δ0 lys2Δ0 ura3Δ0 trp1::URA3 are1::KanMX are2 ::KanMX dga1::loxP GAL1-GFP-LRO1-HIS3*	Roger Schneiter
W303-1A	*MAT***a** *leu2-3,112 ura3-1 trp1-1 his3-11,15 ade2-1 can1-100 GAL SUC2 mal0*	
GHY58	*MAT***a** *can1-100 ade2-1 his3-11,15 leu2-3,112 trp1-1 ura3-1 dpp1Δ::TRP1 Knar lpp1Δ::HIS3/KanR pah1Δ::URA3*	George Carman

All other deletion strains were either single deletions strains obtained from EUROSCARF or were generated by SGA crossing of *MAT***a** single deletion strains with *MAT*α query strains.

Table S2. Plasmids

Plasmid name	Genotype	Reference
pNP302	CEN ARS *URA3,* containing (cytosolic) GFP behind *ADH1* promoter	C. De Virgilio
pYPC1-URA3	*YPC1* replacing GFP in pNP302	This study
pGREG533	CEN6 *HIS3*, kanMX, *GAL1* promoter, N-terminal 7xHA tag	(69)
pBF842	*7xHA-YPC1* (7xHA tag on N-terminus) in pGREG533	(70)
pBF847	CEN *HIS3*, *GAL1* promoter, *YPC1*, in which all cysteines are mutated to Ala or Gly except for C219	(70)
pBF843	*HIS3*, *GAL1* promoter, *YPC1* in which all cysteines are mutated to Ala or Gly except C27	(70)
pSEC7-GFP*	*SEC7-GFP* in CEN *URA3*, *ADH1* promoter	A. Nakano
pGFP-SED5**	GFP-*SED5* in CEN *URA3, TDH3* promoter	A. Nakano

* http://www2.brc.riken.jp/lab/dna/detail.cgi?rdbno=08662;

** http://www2.brc.riken.jp/cache/dna/8658

References used only in Supplemental materials

68. Jacquier N, Choudhary V, Mari M, Toulmay A, Reggiori F, Schneiter R. 2011. Lipid droplets are functionally connected to the endoplasmic reticulum in *Saccharomyces cerevisiae*. J Cell Sci **124**:2424-2437.
69. Jansen G, Wu C, Schade B, Thomas DY, Whiteway M. 2005. Drag&Drop cloning in yeast. Gene **344**:43-51.
70. Ramachandra N, Conzelmann A. 2013. Membrane Topology of Yeast Alkaline Ceramidase YPC1. Biochem J
71. Voynova NS, Vionnet C, Ejsing CS, Conzelmann A. 2012. A novel pathway of ceramide metabolism in *Saccharomyces cerevisiae*. Biochem J **447**:103-114.
72. Bowers K, Stevens TH. 2005. Protein transport from the late Golgi to the vacuole in the yeast *Saccharomyces cerevisiae*. Biochim Biophys Acta **1744**:438-454.
73. Pinto WJ, Srinivasan B, Shepherd S, Schmidt A, Dickson RC, Lester RL. 1992. Sphingolipid long-chain-base auxotrophs of *Saccharomyces cerevisiae*: genetics, physiology, and a method for their selection. J Bacteriol **174**:2565-2574.

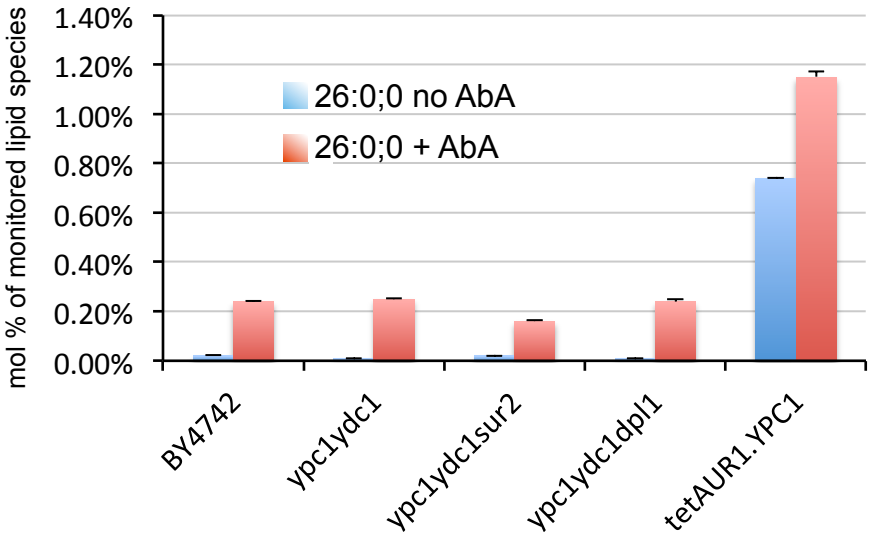

Fig. S1. Increase of non-hydroxylated free VLCFAs in response to AbA in WT cells is not due to futile cycling between LCBs and ceramide. In one of the experiments shown in Fig. 2, *ypc1*Δ*ydc1*Δ, *ypc1*Δ*ydc1*Δ*sur2*Δ and *ypc1*Δ*ydc1*Δ*dpl1*Δ double or triple mutants had been included. The MS data obtained in this experiment showed that free C26:0;0 are elevated upon AbA treatment (0.25 µg/ml, 4 h) although the mutants have no alkaline ceramidases. Means of two technical repeats are shown.

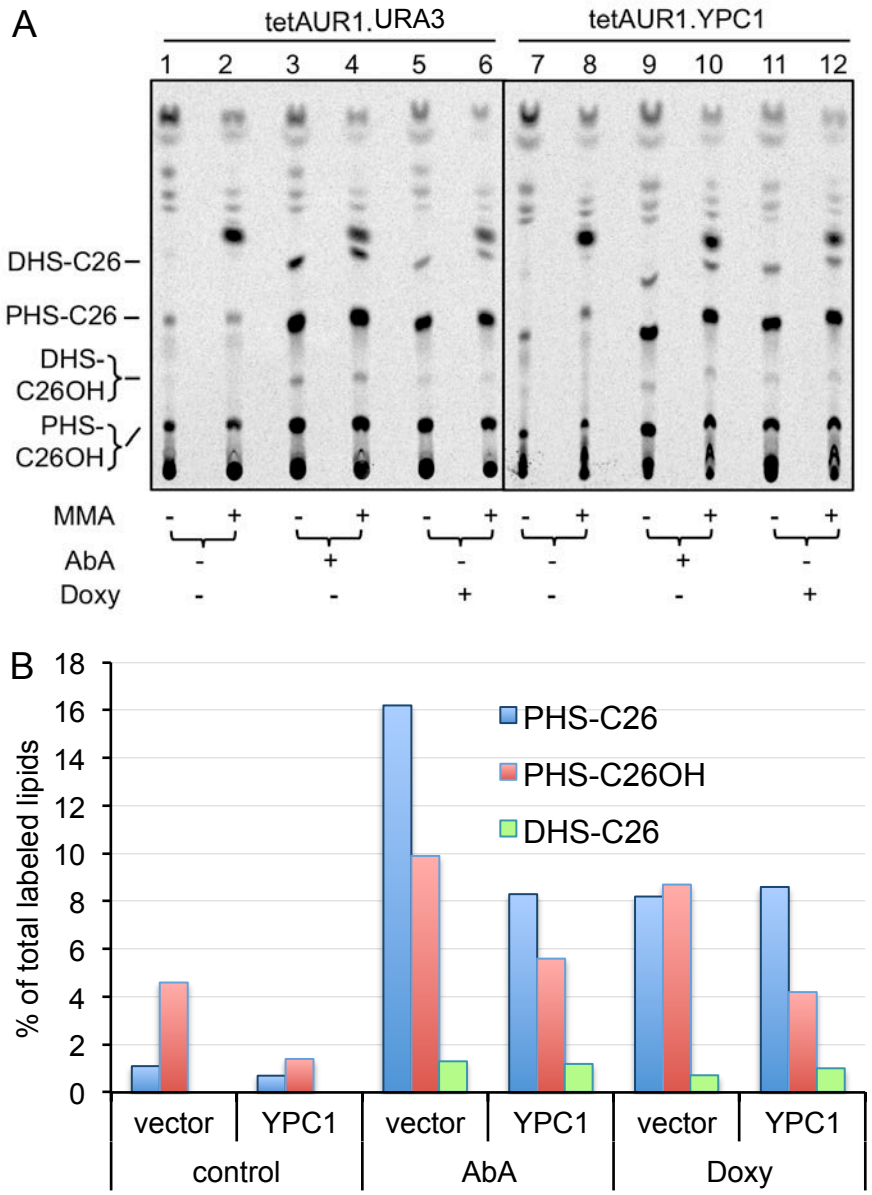

Fig. S2. Overexpression of *YPC1* reduces the ceramide content in living cells. TetAUR1.URA3 or tetAUR1.YPC1 cells were grown with AbA at a final concentration of 3.0 µg/ml for 1 h, or with 10 µg/ml of Doxy for 8 h or used without preliminary treatment (control). Then, cells were metabolically labeled with [^{14}C]serine for 160 min under the same conditions. Lipids were extracted, deacylated with monomethylamine (MMA) or mock incubated (71). (In this type of experiments, the ceramides of WT cells reach plateau levels after 40 min (71)). **A**, Lipids were separated by TLC on silica plates with chloroform/ methanol/glacial acetic acid (90:1:9) as solvent system. Material from an equivalent number of cells was spotted in all lanes. The assignments of DHS-C26, PHS-C26 and PHS-C26OH to distinct bands is based on the presence or absence of major bands of the same mobility in *sur2*Δ*, scs7*Δ and *sur2*Δ*scs7*Δ (not shown). The figure shows one of 3 experiments, which gave similar results. **B**, quantification of data in panel A was achieved by Berthold radioscanning and counts in different ceramide species were expressed as a percentage of total labeled lipids present in the corresponding non-deacylated sample.

Fig. S2

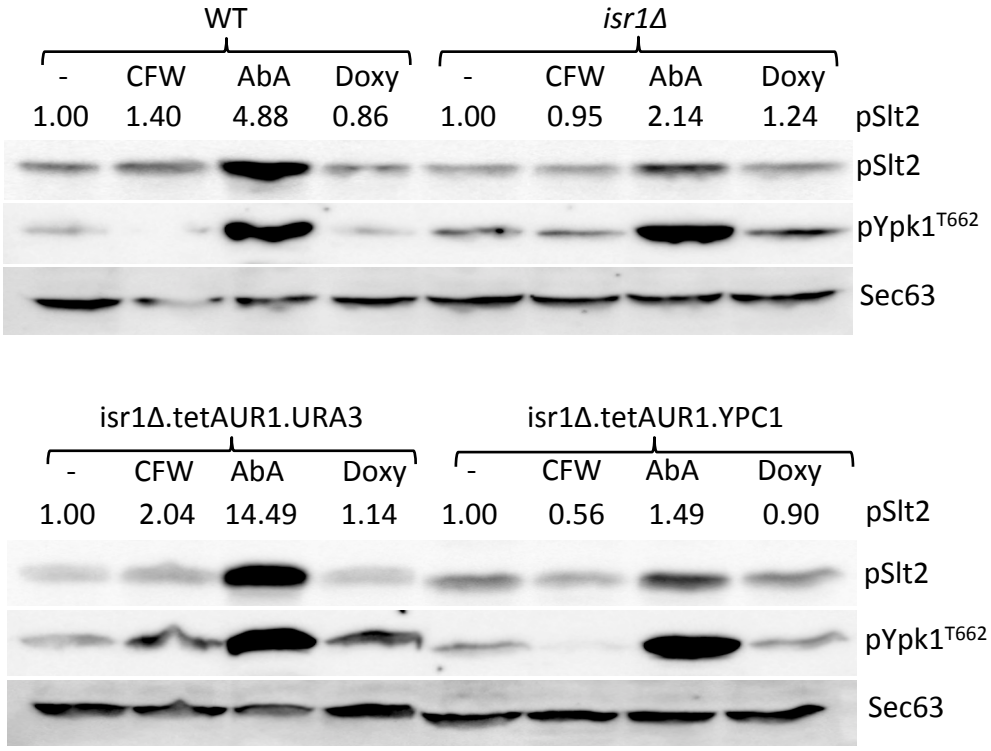

Fig. S3. Detection of activated forms of Slt2 and Ypk1. Activated forms of Slt2 and Ypk1 were detected in indicated strains after treatment with Calcofluor white (CFW), AbA or Doxy exactly as described in Fig. 3C. (Deletion of *ISR1*, a predicted protein kinase of uncharacterized function did not influence the activation of Slt2 and Ypk1).

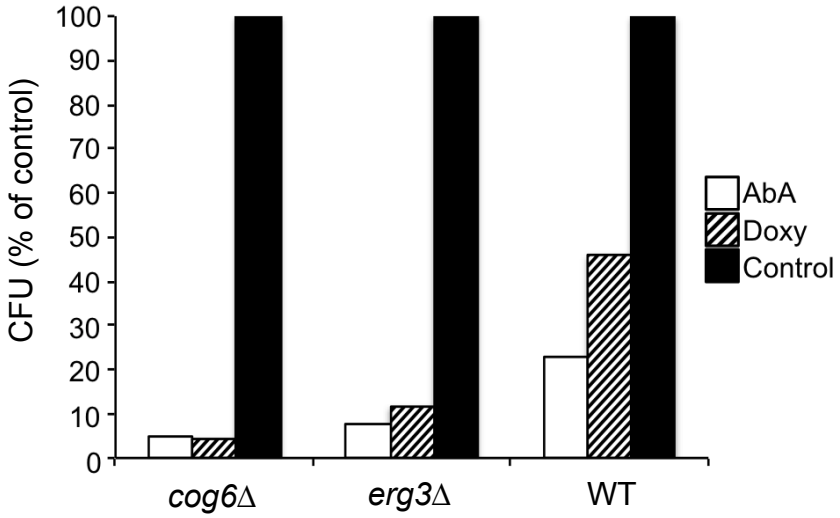

Fig. S4. AbA and Doxy both kill tetAUR1 cells. WT cells, *erg3*Δ and cog6Δ.tetAUR1, two mutants found in preliminary screens to be AbA and Doxy hypersensitive, respectively (Table 2), were grown to exponential phase and then diluted to an OD_{600} of 0.1 in fresh YPD medium supplemented with AbA (0.1 µg/ml), Doxy (5.0 µg/ml) or nothing. Cells were further incubated at 30 ˚C for 3 h in AbA or 7 h in Doxy. Thereafter, colony forming units (CFU) were determined by plating cells on YPD plates. Viability is given as % CFU in comparison with non-treated cells (control).

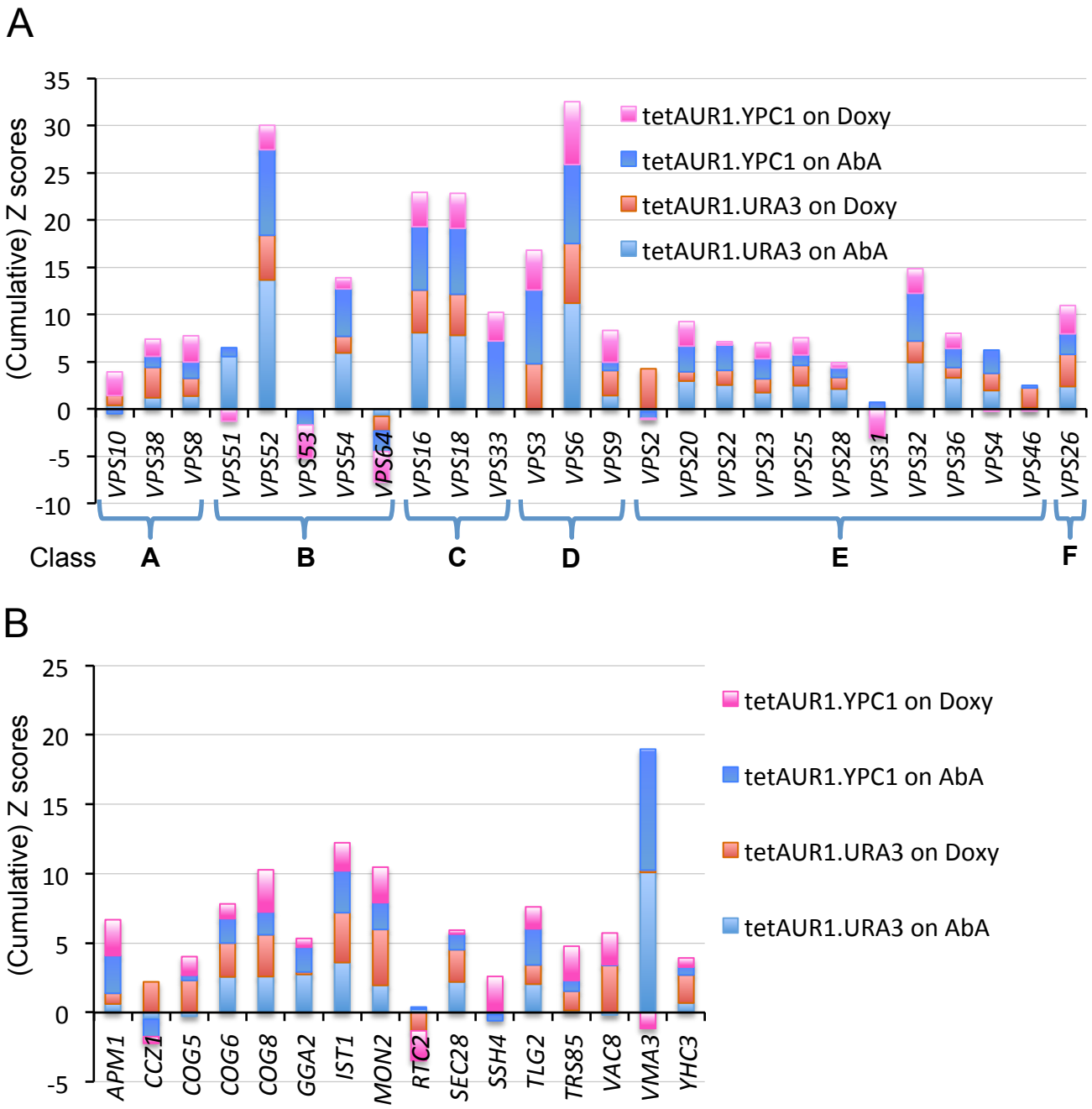

Fig. S5. Z scores of deletions in genes belonging to GO term "vacuolar transport". A, **B**, scores of all deletions yielding at least one significant interaction (| Z score| > 2) in anyone of comparisons 1 – 4 (Fig. 5A) and affiliated to the GO term GO:0007034 "vacuolar transport" according to SGD (http://www.yeastgenome.org/) are plotted. Mutants isolated in the literature as *vps* mutants are shown in panel **A** even if they officially have another name; the others are in panel **B**. In certain strains, one or two colors are lacking; this is most often the case because the quadruplicate colonies were of uneven size and therefore, no Z score was attributed by the ScreenMill software. Most "vacuolar transport" mutants have a positive Z score indicating synthetic sickness. Based on the morphological classification of *vps* mutants (72), most hits belong to class E but the strongest negative interactions are noted with class C and D mutants, whereas class B mutants were less homogeneous, some showing negative scores.

Fig. S5

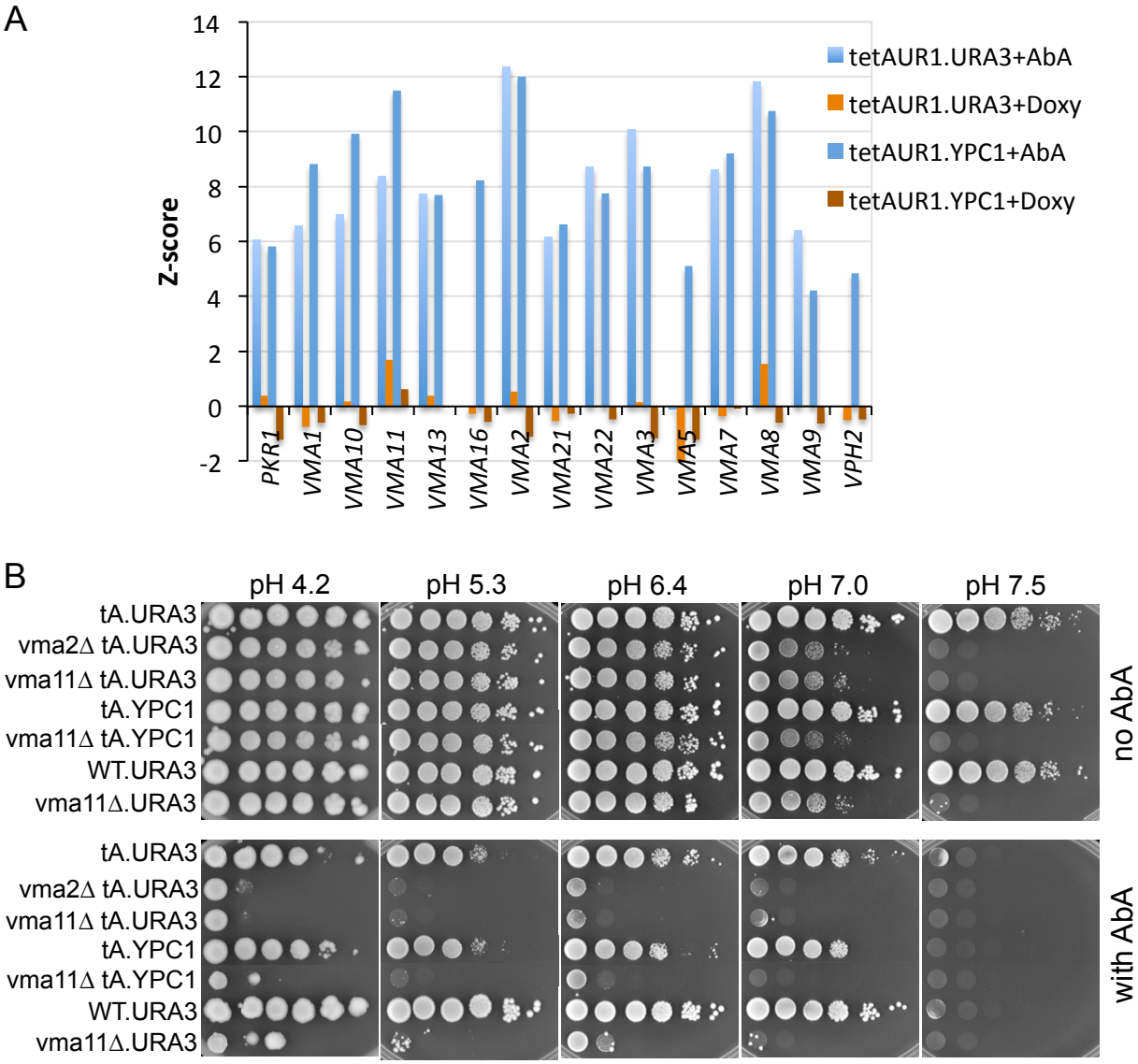

Fig. S6. A, Z-scores of vacuolar acidification mutants on AbA are similar for tetAUR1.URA3 and tetAUR1.YPC1. Z scores for *vma* mutants in comparisons 1 - 4 (Fig. 5A) are shown. For three mutants in the tetAUR1.URA3 background, no values are reported for cells on AbA, for the same reason as mentioned in Fig. S5. **B, low pH of media does not abrogate AbA sensitivity of *vma* mutants.** The *vma* mutants in the tetAUR1 (tA) background were picked and were plated, together with parental strains on complete SC medium (containing 430 µM inositol) buffered with 50 mM sodium succinate and either 50 mM HEPES (pH 7.5) or MES (all other) in presence and absence of 0.03 µg/ml of AbA. Plates were incubated at 30°C for 3 days.

Fig. S6

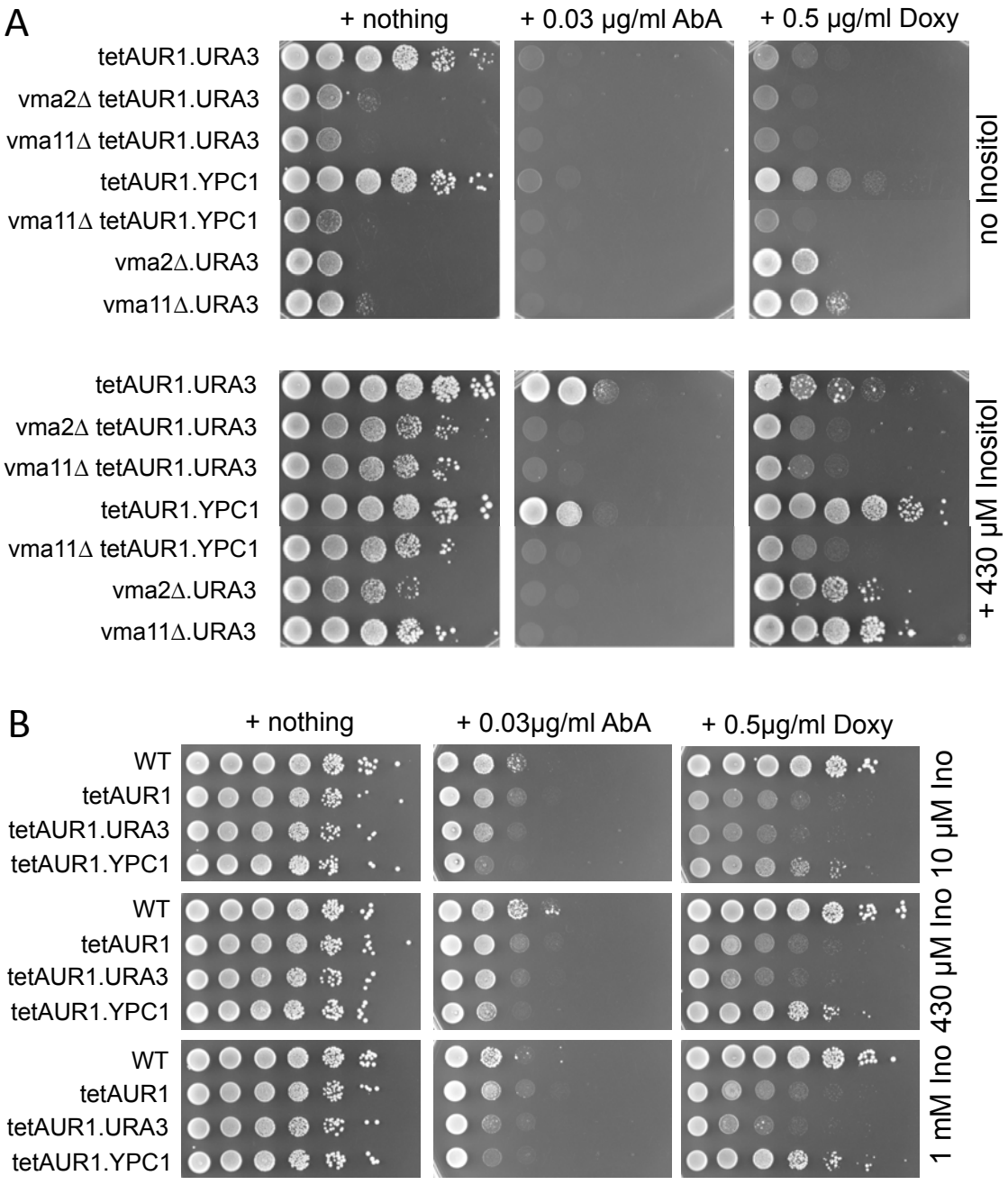

Fig. S7. Hypersensitivity of *vma* mutants to AbA is not caused by inositol auxotrophy. A, cells were grown to exponential phase in SC medium at 30°C. Serial tenfold dilutions were plated on SC media containing the indicated concentrations of drugs and inositol. **B**, BY4742 (WT) or tetAUR1 strains were precultured in SC at 30°C to exponential growth phase. Ten fold serial dilutions were plated on SC having the indicated concentrations of inositol and drugs. Pictures were taken after plates had been at 30°C for 2 days. It had previously been found that very high concentrations of inositol (250 µM) were optimal to sustain growth of *lcb1ΔSLC1-1* cells (73) but with regard to Aur1 repressed cells, high inositol concentrations are apparently of no use. Note that the positive effect of *YPC1* overexpression on growth on Doxy was seen on inositol-free, low inositol or high inositol media.

Fig. S7

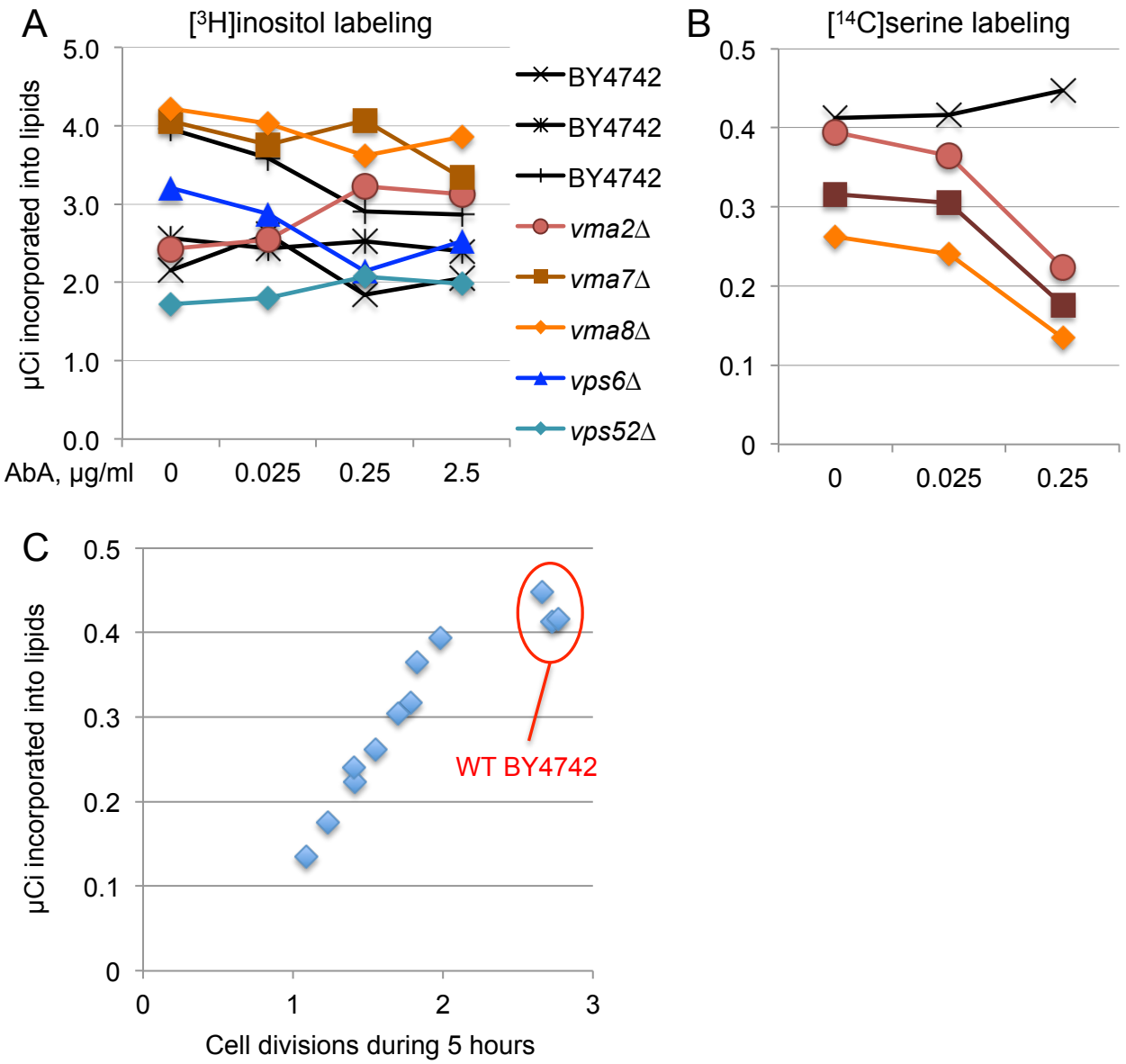

Fig. S8. Influence of AbA on incorporation of [^{3}H]inositol and [^{14}C]serine into lipids. A, total counts (μCi) present in organic solvent extracts of various cell types metabolically labeled during 2 h with 10 μCi of [^{3}H]inositol. **B**, total counts (μCi) present in organic solvent extracts of various cell types metabolically labeled during 5 h with 10 μCi of [^{14}C]serine. Color coding as in panel A. **C**, for the 12 labeling conditions of panel B (4 strains, 3 concentrations of AbA), total counts (μCi) present in organic solvent extracts were plotted as a function of the number of cell divisions cells went through during the 5 h labeling period. WT cells at 0, 0.025 and 0.25 μg/ml of AbA are circled**. D**, for all 12 labelings of panels B and C, the very apolar bands present before and after mild base treatment were calculated as a percentage of the counts present in the TLC lanes of samples not treated with NaOH. While there is a significant increase upon mild base treatment in the intensities of the upper bands of Fig. 6C in most cases, mild base also brings to light a second band with slightly lower mobility, which could be a ceramide but which we have not been able to fully characterize.

Fig. S8

A

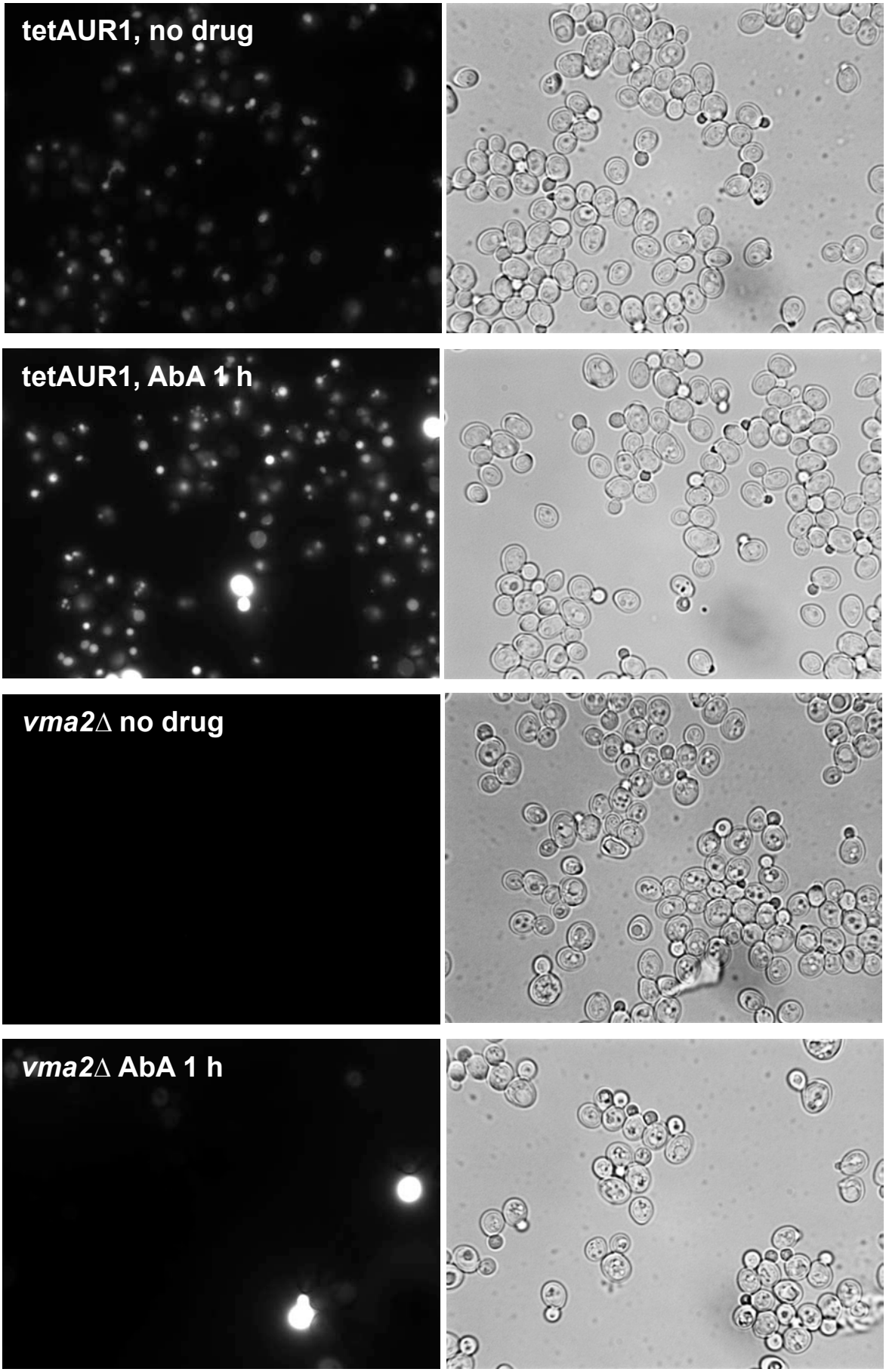

Fig. S9A

B

tetAUR1, no drug

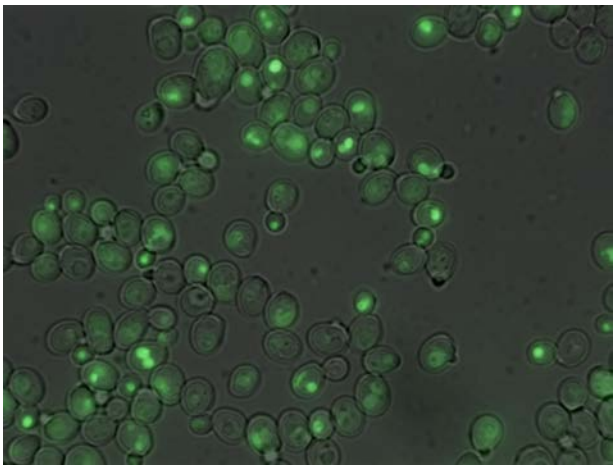

tetAUR1, no drug

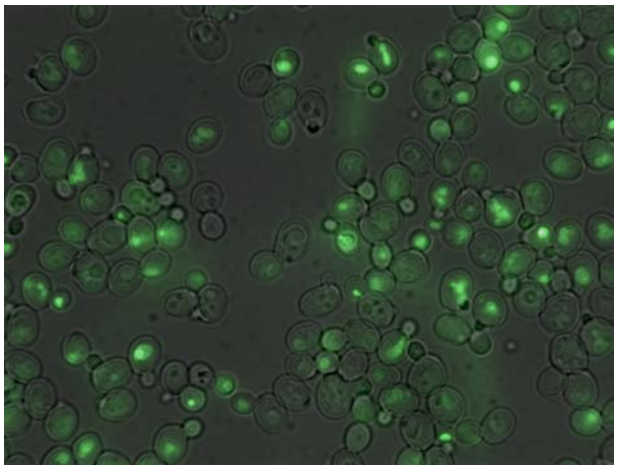

tetAUR1, AbA 1 h

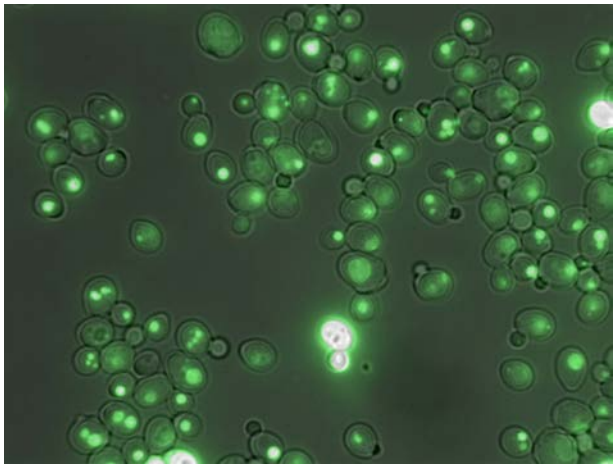

tetAUR1, AbA 1 h

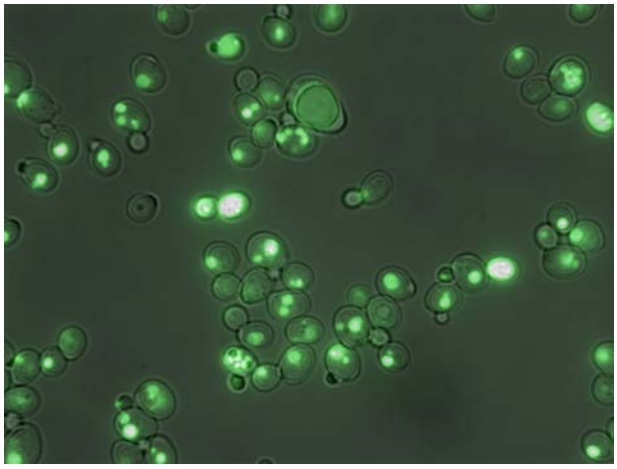

***vma2*∆ no drug**

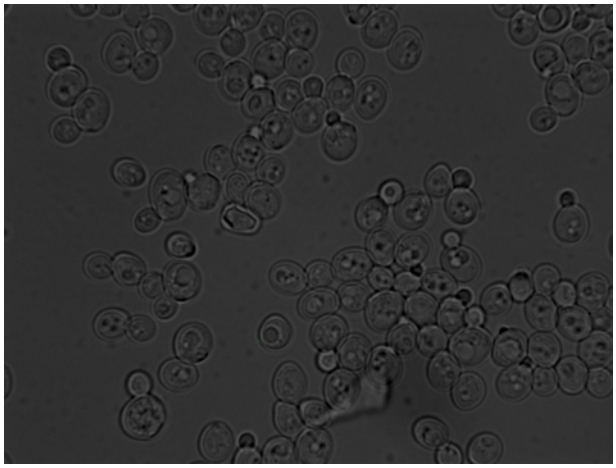

***vma2*∆ AbA 1 h**

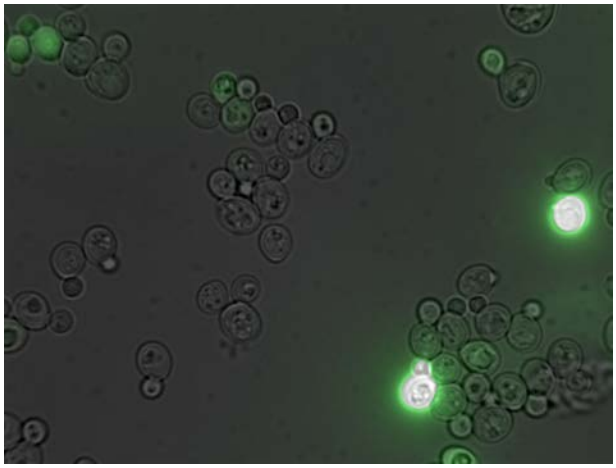

Legend on next page

Fig. S9B

Fig. S9. AbA treatment increases vacuolar and cytosolic Quinacrine accumulation. Exponentially growing tetAUR1 and *vma2*Δ cells were harvested at 0.8 – 1.0 OD_{600} and incubated with or without 0.25 µg/ml AbA at 30°C and pH 6.5 for 1 h, washed, stained with Quinacrine, placed on ice and viewed within 30 min, during which early and late viewings of cells did not show any difference. All pictures were taken under the same conditions and processed with ImageJ using the same window settings (see materials and methods). **A**, the transillumination and fluorescence pictures are shown side by side. **B**, transillumination and fluorescence pictures were merged, whereby the fluorescence pictures, taken with a black and white camera, were rendered green again. The left panels are those already shown in panel A. Pictures of Fig. 7 are taken from these merged pictures.

Fig. S9

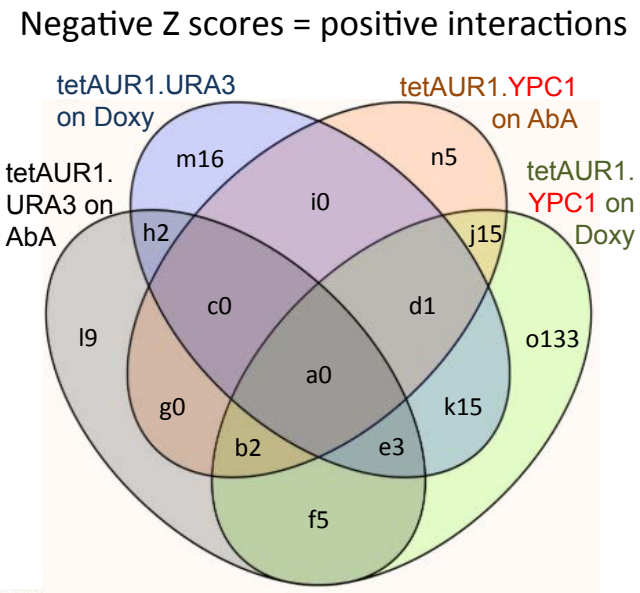

Fig. S10. Deletions enhancing cell growth on AbA and Doxy. Venn diagram analogous to Fig. 5B for gene deletions giving negative Z scores.

Fig. S10

A

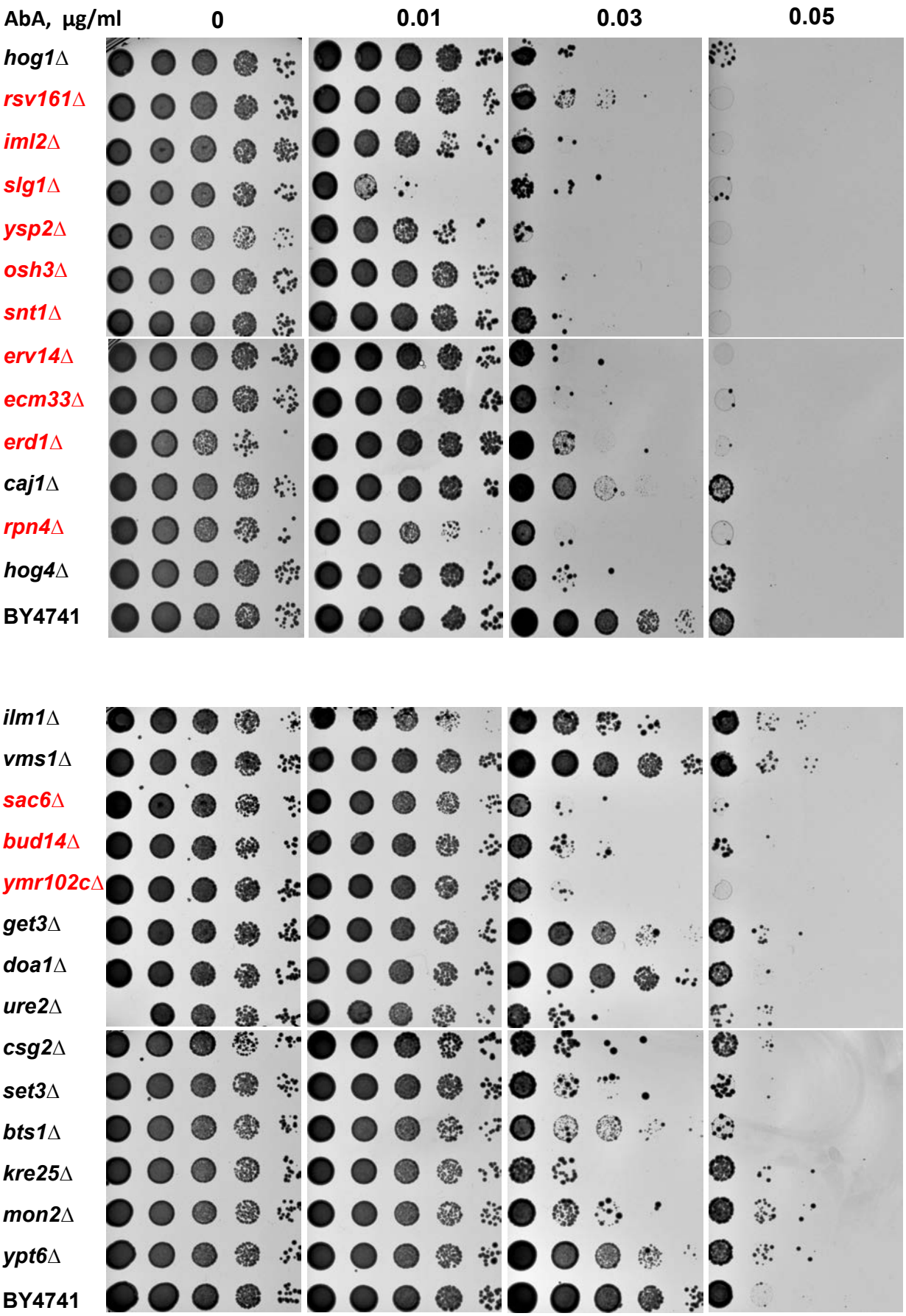
AbA, µg/ml
0
0.01
0.03
0.05
hog1Δ
rsv161Δ
iml2Δ
slg1Δ
ysp2Δ
osh3Δ
snt1Δ
erv14Δ
ecm33Δ
erd1Δ
caj1Δ
rpn4Δ
hog4Δ
BY4741
ilm1Δ
vms1Δ
sac6Δ
bud14Δ
ymr102cΔ
get3Δ
doa1Δ
ure2Δ
csg2Δ
set3Δ
bts1Δ
kre25Δ
mon2Δ
ypt6Δ
BY4741

Fig. S11A

B

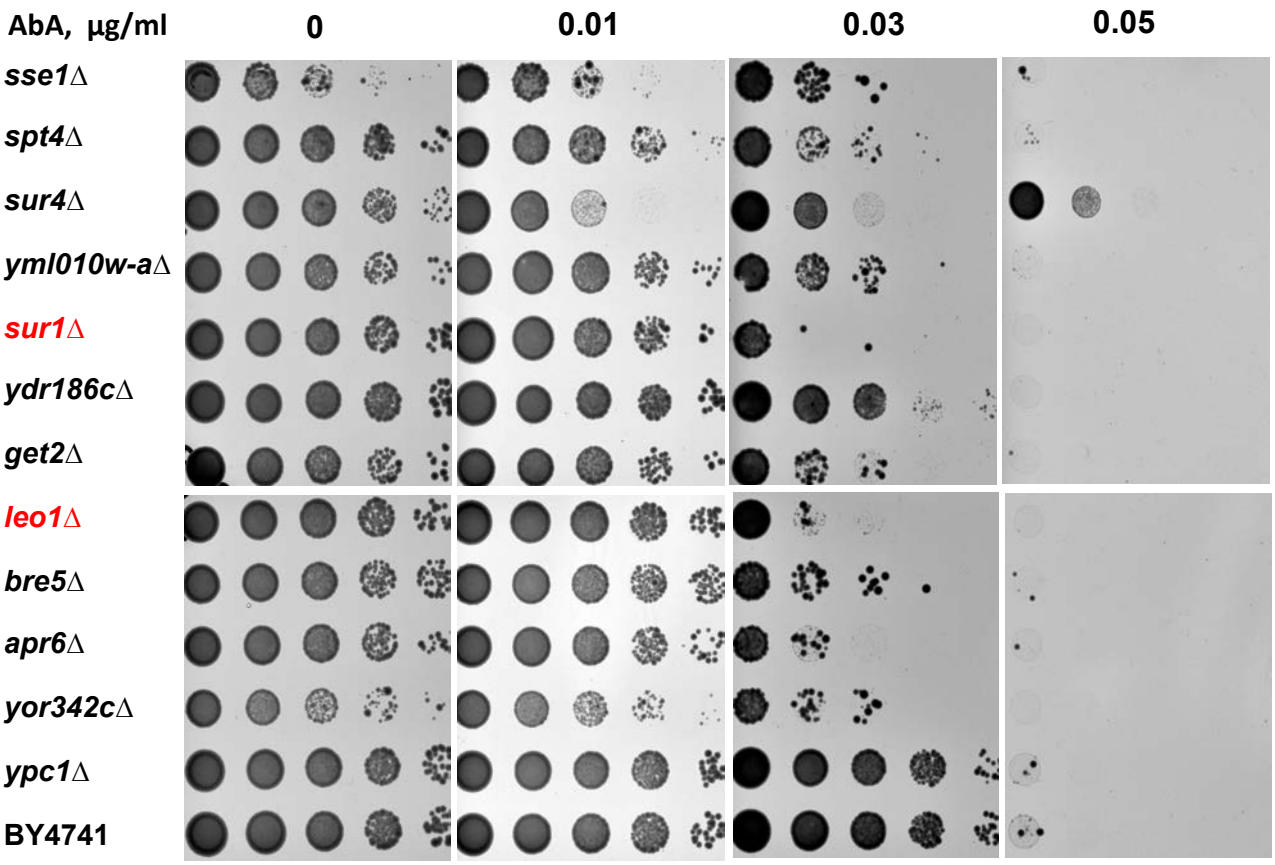
AbA, µg/ml
0
0.01
0.03
0.05
sse1Δ
spt4Δ
sur4Δ
yml010w-aΔ
sur1Δ
ydr186cΔ
get2Δ
leo1Δ
bre5Δ
apr6Δ
yor342cΔ
ypc1Δ
BY4741

Fig. S11B

C

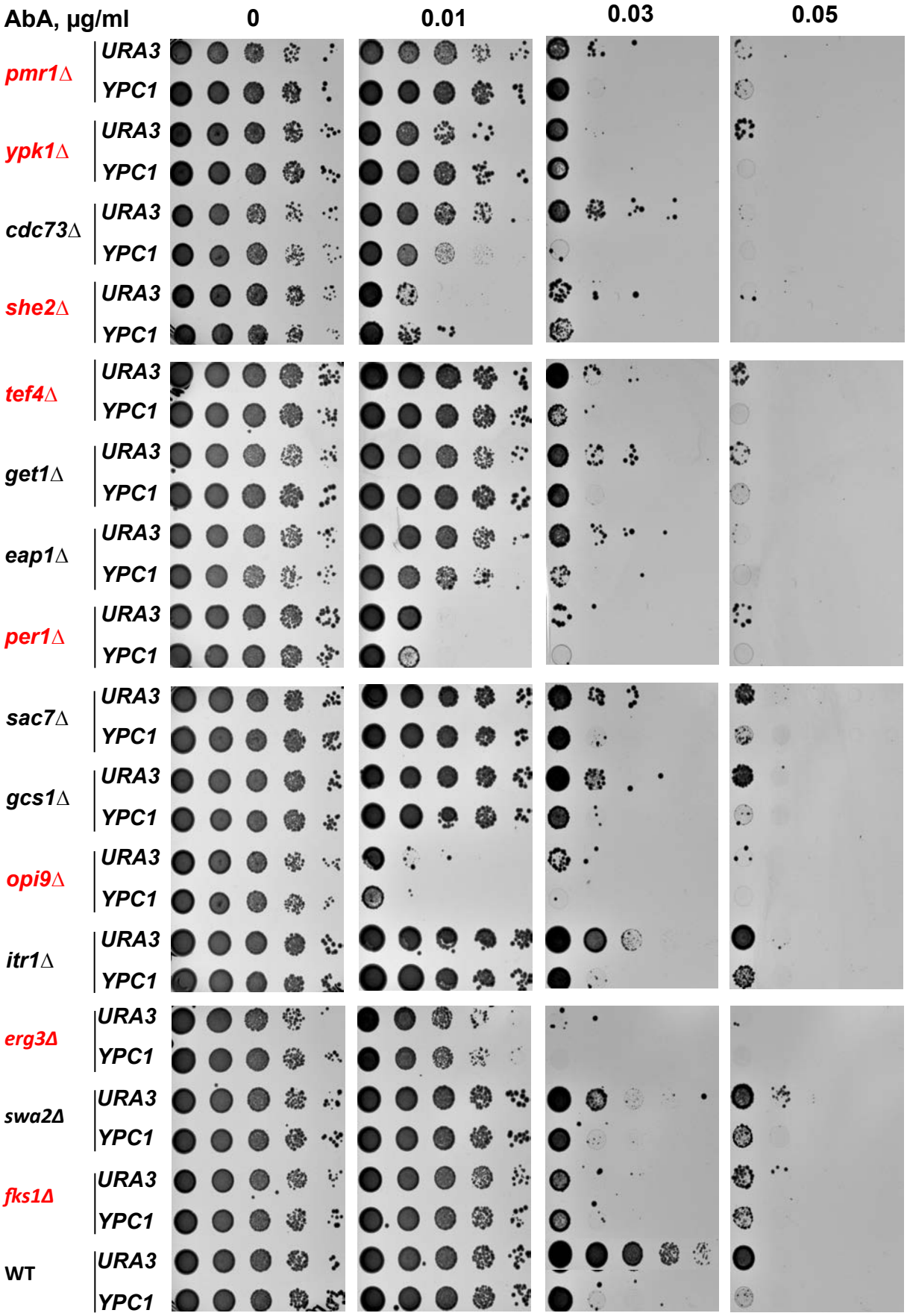
AbA, µg/ml
0
0.01
0.03
0.05
pmr1Δ
ypk1Δ
cdc73Δ
she2Δ
tef4Δ
get1Δ
eap1Δ
per1Δ
sac7Δ
gcs1Δ
opi9Δ
itr1Δ
erg3Δ
swa2Δ
fks1Δ
WT
URA3
YPC1

Fig. S11C

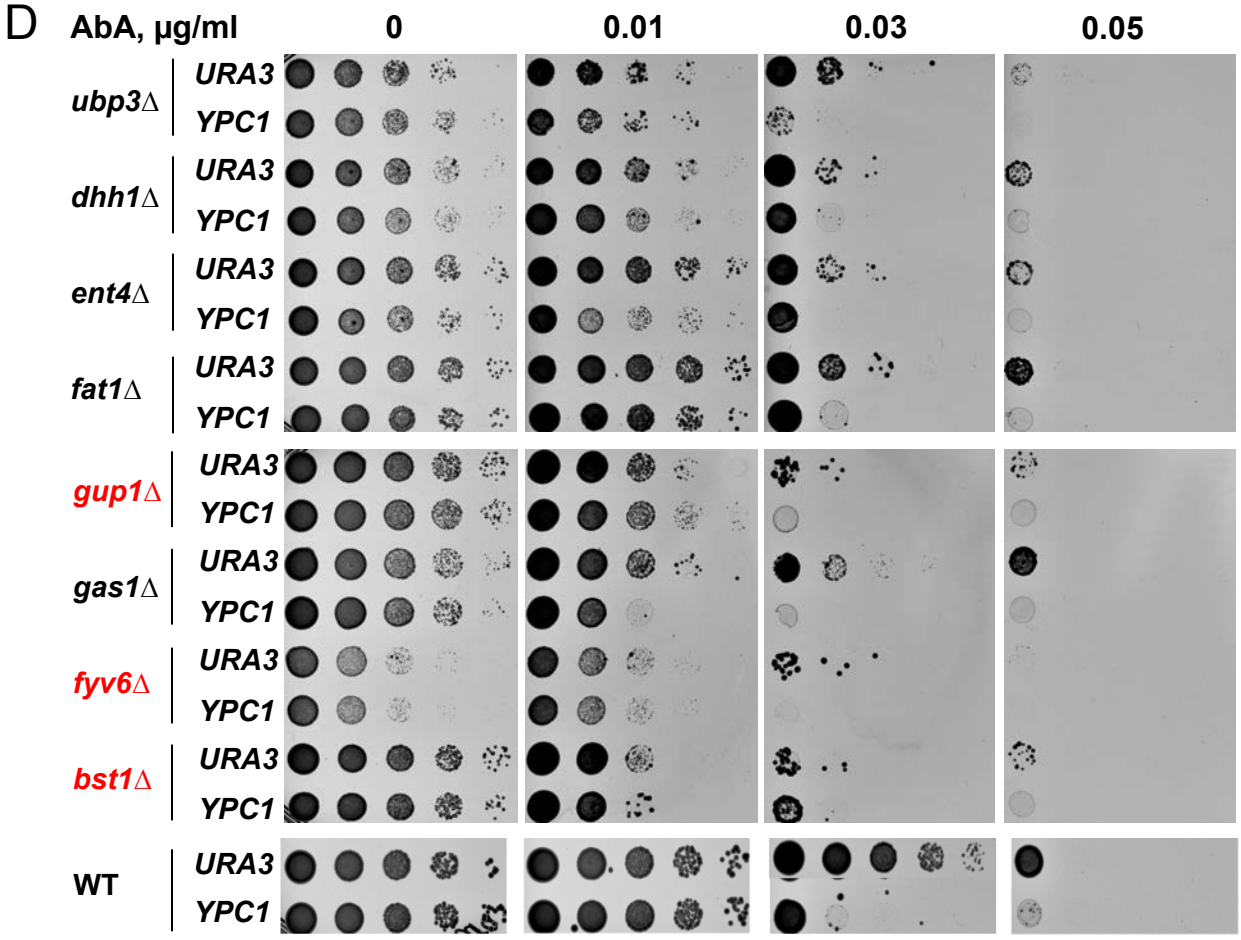

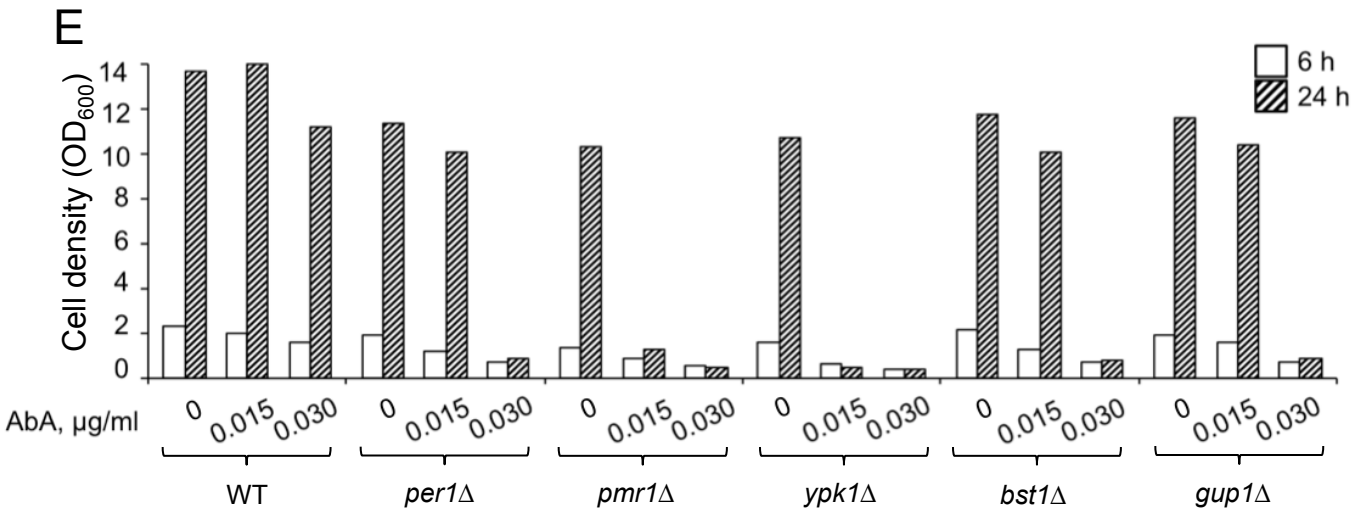

Legend on next page

Fig. S11D, E

Fig. S11. Validation of genetic interactions found in preliminary screens by serial dilution plating assay. In preliminary high throughput SGA screens the library containing 4849 G418 resistant strains, each one deleted in a single non-essential gene, was robotically crossed with BY4742 (FBY5313, panels **A**, **B**), or with BY4742 harboring pYPC1-URA3 or the control vector pNP302 (FBY5332 and FBY5333, panels **C**, **D**). Haploid progeny was selected on G418 plus 0 or 0.03 μg/ml of AbA. To validate SGA findings, 62 mutants of interest showing significant sensitivity to AbA were selected and tested by serial dilution growth assays on SC media containing the indicated concentrations of AbA. In this way, 26 out of 62 strains were found to be AbA hypersensitive (red) and reported in Table 2.
These serial dilution assays also confirmed that *YPC1* overexpression can aggravate AbA toxicity as had been found in WT cells (Figs. 3A, 4A): When tested in parallel (panels **C**, **D**), 17 of 23 *YPC1* overexpressing strains grew less well on AbA than the corresponding strain harboring the control vector. This was also true for 5 out of the 11 AbA hypersensitive strains whereas in the other 6, the mutations had abolished the difference between *YPC1* expressing and control cells. **E**, indicated strains were grown till early exponential phase in liquid media (YPD) and then diluted in the same medium supplemented with AbA at concentrations of 0.015 μg/ml and 0.030 μg/ml or without the drug at a density (OD_{600}) of 0.3 and incubated at 30 ˚C. Density (OD_{600}) was measured at 6 and 24 h.

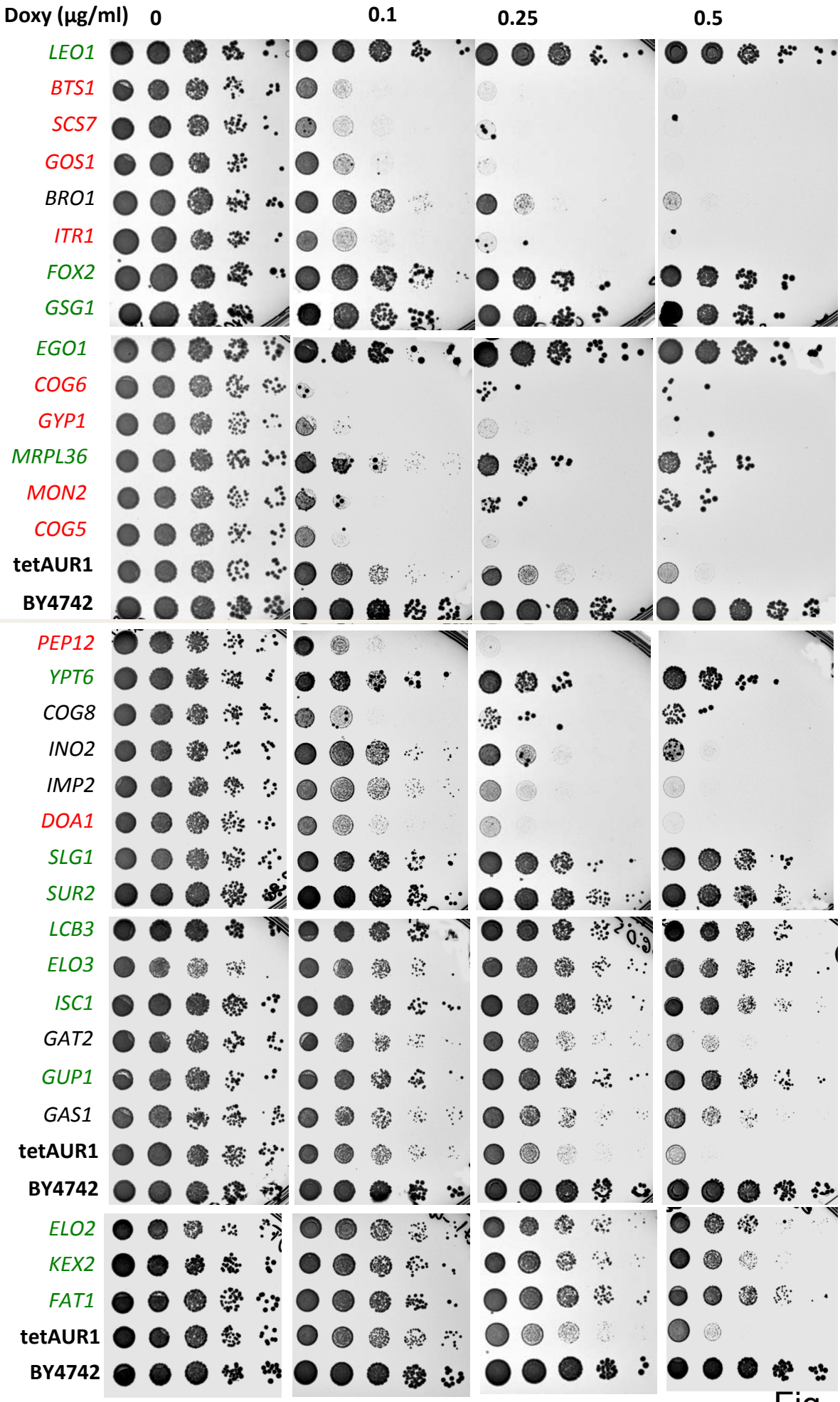

Legend on next page

Fig. S12

Fig. S12 Validation of genetic interactions found in preliminary screens by serial dilution plating assay. In other preliminary screens, the tetAUR1 strain was robotically crossed with the deletion library and resulting haploids at the last stage of selections were plated on a Doxy concentration of 0.1 µg/ml, a concentration that did not greatly affect the growth of the parental tetAUR1 strain. Ten fold dilutions of some of the most sensitive or most resistant double mutants obtained in the screen were taken form the fresh plates and grown to exponential phase and then plated in tenfold dilutions onto YPD plates containing various concentrations of Doxy. Plates were incubated during 2 days at 30°C. The 10 deletion strains considered to be hypersensitive and the 15 considered hyper-resistant in comparison to the parental tetAUR1 strain are in red or green, respectively, and are reported in Table 2. The Doxy hyper-resistant clones of Table 2 were significantly enriched in lipid biosynthesis terms GO such as sphingolipid biosynthetic process (GO:0030148, P value = 4.90E-05). These preliminary screens on Doxy confirmed that *scs7*Δ are hypersensitive, *elo3*Δ and *sur2*Δ hyper-resistant to Aur1 repression as described previously (39, 40).

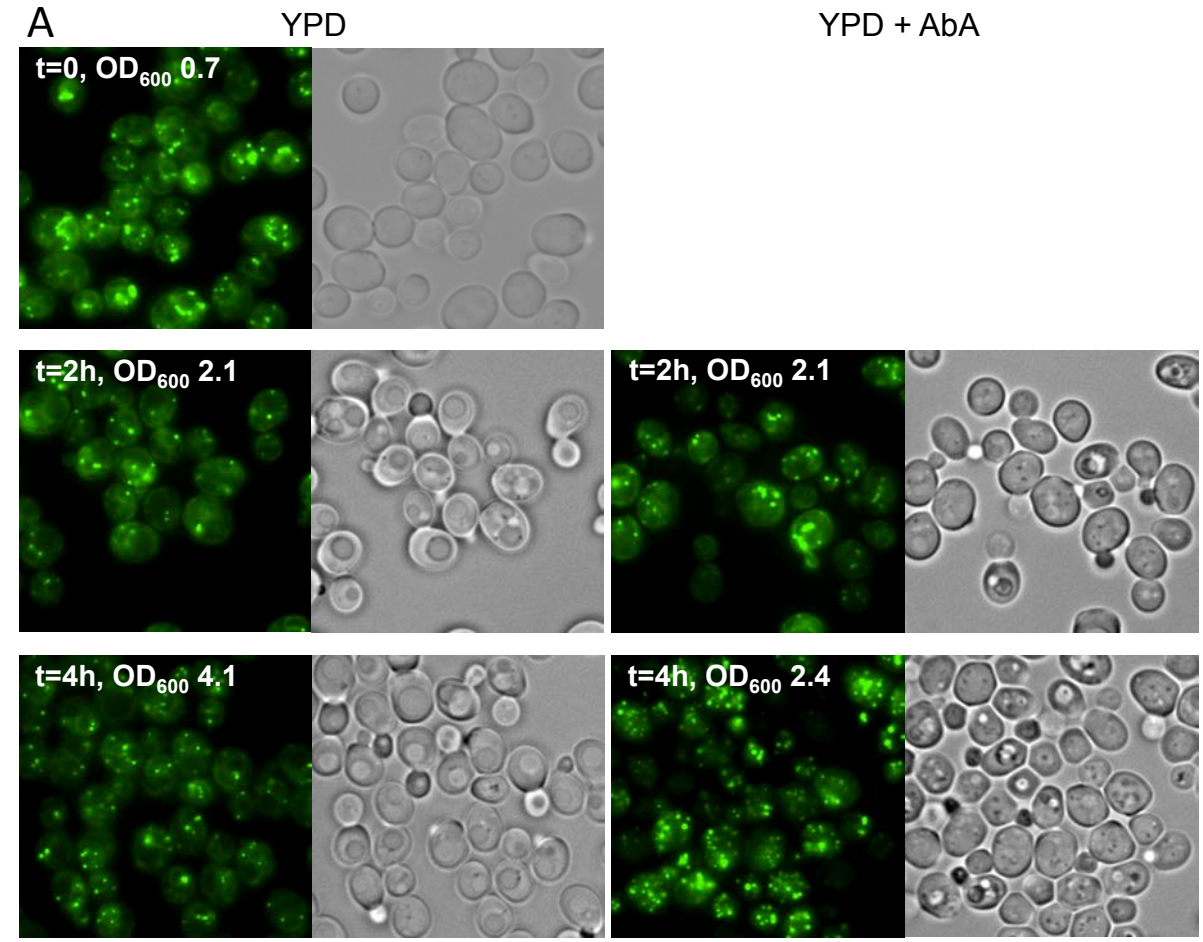

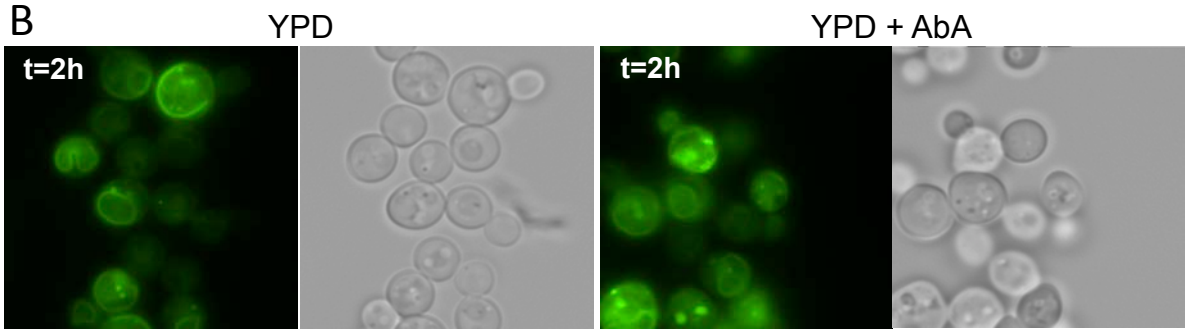

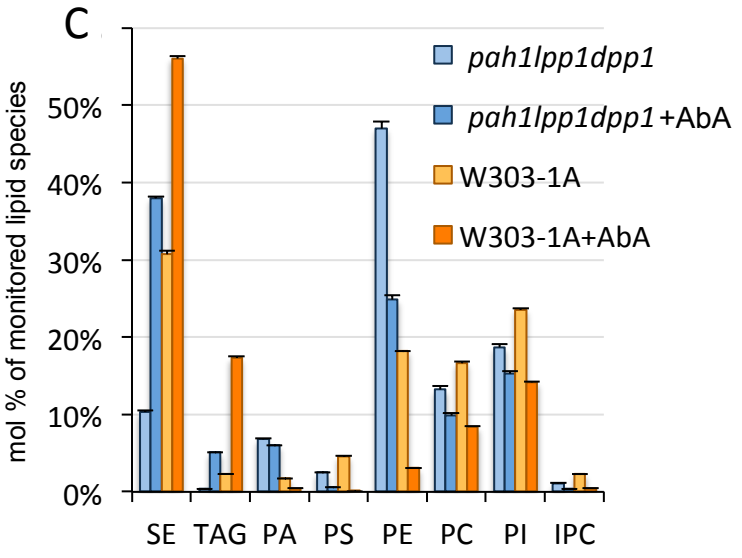

Legend on next page

Fig. S13

Fig. S13. Incubation with AbA increases lipid droplets. A, BY4742 WT and **B**, *pah1*Δ*lpp1*Δ*dpp1*Δ (GHY58) were grown to exponential phase and further incubated with or without AbA (0.25µg/ml) for 0, 2 or 4 hours. At indicated time points cells had reached the indicated density (OD_{600}) and were stained with BODIPY 493/503 for staining of lipid droplets as described (68). **C**, MS analysis of lipid extracts from exponentially growing WT (W303-1A) or mutant (GHY58) cells before and after incubation with 0.25µg/ml AbA for 4 hours. Means of two technical replicates are shown. The same trends in lipid profiles as documented in Fig. 8A are also observed here in the genetic background of W303.

Fig. S13

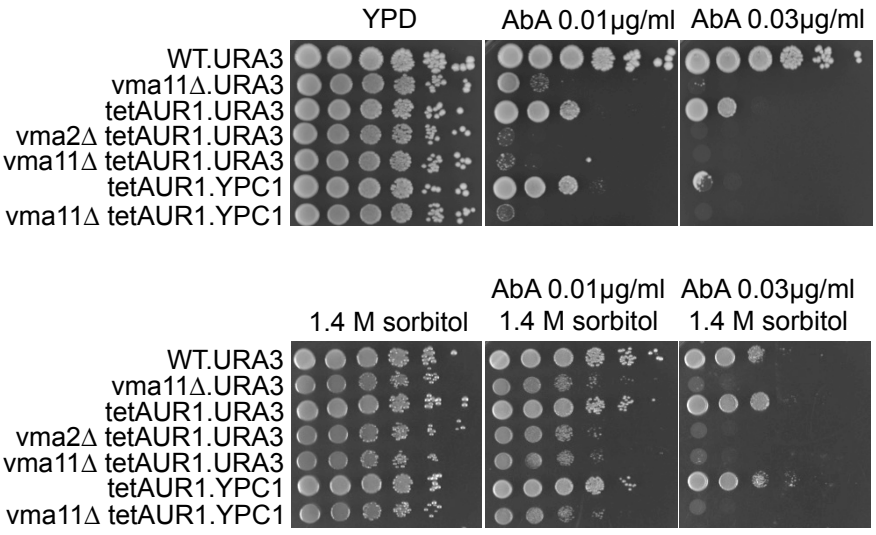

Fig. S14. Growth of *vma* mutants on low concentrations of AbA is helped by osmotic support. Ten fold dilutions of *vma* mutants in the BY4742 or tetAUR1 background were spotted onto YPD plates with or without sorbitol.

Fig. S14